Analysis of Microstrip Line to Waveguide End Launchers

T. Q. HO AND YI-CHI SHIH, MEMBER, IEEE

Abstract—**An analysis of a microstrip line to waveguide end launcher is presented. The expression for input impedance is derived through the self-reaction concept with the assumption of a sinusoidal current distribution existing in the conductor loop. Three different cases of end launchers are computed for their corresponding input impedances. Comparison between calculated and measured input return loss of an end launcher shows good agreement between theory and experiment at *Ka*-band frequencies.**

I. INTRODUCTION

THE MICROSTRIP LINE to waveguide end launcher is an important device in microwave circuits used to couple power from a waveguide to an input of a microstrip integrated circuit. In a microstrip circuit, where waveguide is specified for the input and output ports, the circuit requires a good waveguide to microstrip transition. Waveguide to microstrip transitions exist in several forms; however, the two transitions commonly known are the *E*-plane and the finline types [1], [2]. In the *E*-plane waveguide to microstrip transition, a probe which is formed by the conducting metal on the substrate is inserted into an operating waveguide. A back-short is then placed at an optimum location away from the center of the microstrip probe to maximize the coupling power extracted from the waveguide to an input microstrip line. The *E*-plane waveguide to microstrip transition is a noncollinear transition.

A second type of transition is the finline waveguide to microstrip transition. In the circuit, the gradually tapered metal fins on both sides of a dielectric substrate are used to concentrate and rotate the electric field into a parallel line within the waveguide. The fins are then fed into a quarter-wave balun transformer to converge the field from a symmetrical line into an asymmetrical microstrip line. The finline waveguide to microstrip transition is an in-line waveguide feed type. However, due to the complexity of the finline circuit structure, the usage of this type of transition is limited. In this paper we will introduce a new type of transition, known as a microstrip line to waveguide end launcher. The end launcher circuit can be fabricated using a printed-circuit board placed inside a waveguide. The L-shaped metal loop is used to launch the power directly from an in-line waveguide to an input microstrip line. For high-frequency operation, this type of transition has a greater potential to become an ideal waveguide to microstrip transition due to the simplicity of the circuitry.

The theories of waveguide end launchers are very well documented; the major effort has been applied to coaxial lines. Collin [3] has analyzed a transition in which its center conductor is bent into a semicircular loop. Harrington [4] found a method of determining an equivalent network of a junction between the waveguide and a coaxial line and determined the input impedance through a stationary formula. Das *et al.* [5], [6] have presented an analysis of the concentric and offset cases of coaxial line to waveguide end launchers. Until now, the analysis of the microstrip line to waveguide end launcher has not been available. As microstrip circuits become popular at microwave frequencies, it is important to develop a theory so that the end launcher may be designed.

This paper introduces an analytical method using the self-reaction concept to obtain the input impedance of a microstrip line to waveguide end launcher. Three different cases of end launchers are evaluated to determine their input impedances. A comparison between the calculated and measured input return loss of an end launcher is presented to verify the agreement between theory and experimental data.

II. FORMULATION

The structure to be analyzed is shown in Fig. 1, where a printed-circuit board is placed inside a dominant TE_{10} waveguide and the current loop on the circuit board is driven from a generator through a microstrip line. In the analysis, the current loop is divided into two different sections: the z-directed current component extends from the plane $z = 0$ to $z = z_1$, while the x-directed component extends from $x = 0$ to $x = x_1$. The current is continuous at the connecting point $x = x_1$ and $z = z_1$. The perfect ground plane formed by the waveguide side walls is located at $x = 0$ and a, $y = 0$ and b, and $z = 0$. The current strip is assumed to be infinitely thin in the y direction, and it is sufficiently narrow that the current distribution does not vary appreciably in the transverse direction with respect to the metal strip. In addition, for simplicity of analysis, the effects of the exciting aperture at the plane $z = 0$ are neglected. The analysis procedure is outlined in the following steps:

Step 1) Determine the dyadic Green's function $G(x, y, z/x', y', z')$ for the region inside the waveguide.

Manuscript received April 30, 1987; revised October 2, 1987.

T. Q. Ho is with Hughes Aircraft Company, Space & Communications Group, Los Angeles, CA 90009.

Y. C. Shih is with Hughes Aircraft Company, Industrial Electronics Group, Torrance, CA 90509.

IEEE Log Number 8718869.

0018-9480/88/0300-0561$01.00

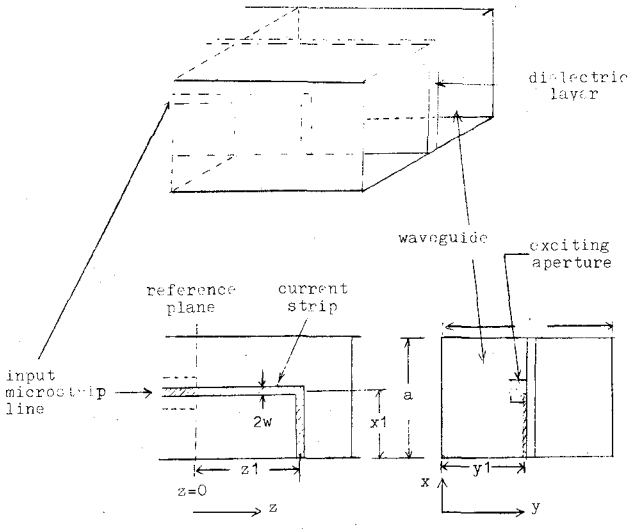

Fig. 1. Geometry of a microstrip line-to-waveguide end launcher.

The Green's function is expressed in a form of orthogonal functions defined by the boundary conditions.

Step 2) Assume the current densities. J_z is the current distribution in the z direction and J_x is the current distribution in the x direction.

Step 3) Determine the excited magnetic vector potentials A_z and A_x, and then the electric fields E_z and E_x.

Step 4) Develop an expression for the input impedance of the end launcher seen by the microstrip line at the feeding point.

Step 5) Obtain an expression for the reflection coefficient of the end launcher in a back-to-back configuration.

A. The Dyadic Green's Function

Because the current is directed in both the z and x directions, there will be two Green's functions existing for the problem. The dyadic Green's functions are the solutions of the following inhomogenous equation:

$$\nabla \times \nabla \times \bar{\bar{G}}(x, y, z/x', y', z') - k^2 \bar{\bar{G}}(x, y, z/x', y', z') = \bar{\bar{I}}\delta(x-x')\delta(y-y')\delta(z-z') \quad (1)$$

for the given boundary conditions [7]. $\bar{\bar{I}}\delta(x-x')\delta(y-y')\delta(z-z')$ represents the unit dyad at location $x=x'$, $y=y'$, and $z=z'$. The complete Green's functions for the z and the x directions are given respectively by

$$G_{zz}(x, y, z/x', y', z') = \sum_{n=1}^{\infty}\sum_{m=1}^{\infty} \frac{1}{2ab\gamma_{mn}} \sin\left(\frac{n\pi x}{a}\right)\sin\left(\frac{m\pi y}{b}\right) \cdot \sin\left(\frac{n\pi x'}{a}\right)\sin\left(\frac{m\pi y'}{b}\right) e^{\pm\gamma_{mn}(z-z')} \quad (2a)$$

$$G_{xx}(x, y, z/x', y', z') = \sum_{n=0}^{\infty}\sum_{m=1}^{\infty} \frac{\delta_n}{ab\gamma_{mn}} \cos\left(\frac{n\pi x}{a}\right)\sin\left(\frac{m\pi y}{b}\right) \cdot \cos\left(\frac{n\pi x'}{a}\right)\sin\left(\frac{m\pi y'}{b}\right) e^{\pm\gamma_{mn}(z-z')} \quad (2b)$$

where

$$\gamma_{mn} = \sqrt{\left(\frac{n\pi}{a}\right)^2 + \left(\frac{m\pi}{b}\right)^2 - k^2} \quad (3a)$$

$$k = \frac{2\pi\sqrt{\epsilon_{\text{eff}}}}{\lambda}. \quad (3b)$$

Here λ is the free-space wavelength and ϵ_{eff} is the effective dielectric constant. $\delta_n = 1$ for the dominant mode, and $\delta_n = 2$ otherwise. γ_{mn} is the propagation constant of the mode inside the waveguide; it is purely imaginary for the dominant mode, and real for the higher order mode. The $+$ and $-$ signs in the exponential terms in (2a) and (2b) correspond to $z < z'$ and $z > z'$, respectively. The prime variables x', y', z' represent the source points, while the unprimes represent the field points.

B. Current Density

In the coordinate system shown in Fig. 1, the metal strip is extended from the point $(x_1, y_1, 0)$ to the point $(0, y_1, z_1)$. At the point $(0, y_1, z_1)$ the current strip is shorted to the side wall of the waveguide. The current strip is considered to be narrow so that we can neglect the current variation in the transverse direction. For the purpose of calculation, the end launcher probe is considered a linear antenna radiating into a waveguide. The current is continuous at the point (x_1, y_1, z_1). The distribution of the trial current in the strip is assumed to have a sinusoidal distribution of the form

$$\vec{J}_z = \vec{a}_z I_0 \cos(k(z_1 + x_1 - z))\delta(y - y_1), \quad 0 \le z \le z_1 \text{ and } x_1 - w \le x \le x_1 + w \quad (4a)$$

$$\vec{J}_x = \vec{a}_x I_0 \cos(kx)\delta(y - y_1), \quad 0 \le x \le x_1 \text{ and } z_1 - w \le z \le z_1 + w \quad (4b)$$

where $\vec{a}_z$ and $\vec{a}_x$ are the unit vectors in the z and the x directions, respectively. I_0 is the magnitude of the input current and k is the medium wavenumber.

C. The Magnetic Vector Potentials and the Electric Fields

The magnetic vector potential due a current distribution is defined as

$$A = \int_{v'} \bar{\bar{G}}(x, y, z/x', y', z') \cdot \vec{J}(x', y', z')\, dV'. \quad (5)$$

The integration is carried over the source point x', y', z'. The Green's functions and the current distributions are given in (2a), (2b), (4a), and (4b). The magnetic vector potentials A_z and A_x are derived by application of the

image principle [8]:

$$\vec{A}_z = \vec{a}_z \sum_{n=1}^{\infty}\sum_{m=1}^{\infty} \frac{I_0}{2ab\gamma_{mn}} \sin\left(\frac{n\pi x}{a}\right)\sin\left(\frac{m\pi y}{b}\right) \cdot\left[\int_0^b\int_0^a \cos\left(\frac{n\pi x'}{a}\right)\cos(kx') \cdot\sin\left(\frac{m\pi y'}{b}\right)\delta(y'-y_1)\,dx'dy' \cdot\left(\int_{-\infty}^{0} e^{\pm\gamma_{mn}(z-z')}\cos\left(k(z_1+x_1+z')\right)dz' + \int_0^{\infty} e^{\pm\gamma_{mn}(z-z')}\cos\left(k(z_1+x_1-z')\right)dz'\right)\right] \quad (6a)$$

and

$$\vec{A}_x = \vec{a}_x \sum_{n=0}^{\infty}\sum_{m=1}^{\infty} \frac{I_0\delta_n}{ab\gamma_{mn}} \cos\left(\frac{n\pi x}{a}\right)\sin\left(\frac{m\pi y}{b}\right) \cdot\left[\int_0^b\int_0^a \cos\left(\frac{n\pi x'}{a}\right)\cos(kx') \cdot\sin\left(\frac{m\pi y'}{b}\right)\delta(y'-y_1)\,dx'dy' \cdot\left(-\int_{-\infty}^{0} e^{\pm\gamma_{mn}(z-z')} + \int_0^{\infty} e^{\pm\gamma_{mn}(z-z')}\right)dz'\right]. \quad (6b)$$

Now that the analytical forms of the magnetic vector potential A_z and A_x have been obtained, the next step is to perform the integrations of (6a) and (6b). The variables dx', dy', dz' are integrated from 0 to a, 0 to b, and $-\infty$ to $+\infty$, respectively. The magnetic vector potentials are now reduced to their closed-form expressions, as follows:

$$\vec{A}_z = \vec{a}_z \sum_{n=1}^{\infty}\sum_{m=1}^{\infty} \frac{I_0}{ab\gamma_{mn}(k^2+\gamma_{mn}^2)} \sin\left(\frac{n\pi x_1}{a}\right)\sin\left(\frac{m\pi y_1}{b}\right) \cdot\sin\left(\frac{n\pi x}{a}\right)\sin\left(\frac{m\pi y}{b}\right)\left[e^{-\gamma_{mn}z} \cdot\sin\left(k(z_1+x_1)\right) - e^{-\delta_{mn}z_1} \cdot\left(\gamma_{mn}\cos(kx_1)+k\sin(kx_1)\right)\cosh(\gamma_{mn}z)\right] \quad (7a)$$

$$\vec{A}_x = \vec{a}_x \sum_{n=0}^{\infty}\sum_{m=1}^{\infty} \frac{2I_0\delta_n k}{ab\gamma_{mn}} \cos\left(\frac{n\pi x}{a}\right)\sin\left(\frac{m\pi y}{b}\right)e^{-\gamma_{mn}z} \cdot\sin\left(\frac{m\pi y_1}{b}\right)\sinh(\gamma_{mn}z_1) \cdot\left[\frac{\frac{n\pi}{ak}\cos(kx_1)\sin\left(\frac{n\pi x_1}{a}\right) - \sin(kx_1)\cos\left(\frac{n\pi x_1}{a}\right)}{k^2-\left(\frac{n\pi}{a}\right)^2}\right]. \quad (7b)$$

Here the term $\exp(-\gamma_{mn}z)$ represents the wave propagating in the positive z direction. Since the expressions of the magnetic vector potentials have been derived, the excited E fields due to the current arms J_z and J_x can be determined through the following relations:

$$E_z = \frac{1}{j\omega\epsilon_0}\left(\frac{\partial^2 A_z}{\partial z^2} + k^2 A_z\right) \quad (8a)$$

$$E_x = \frac{1}{j\omega\epsilon_0}\left(\frac{\partial^2 A_x}{\partial x^2} + k^2 A_x\right). \quad (8b)$$

E_z is the z-directed electric field due to the z-directed current, and E_x is the x-directed electric field due to the x-directed current component. Substitution of the magnetic vector potentials A_z and A_x from (7a) and (7b) into (8a) and (8b) yields the expressions for E_z and E_x given by

$$\vec{E}_z = \vec{a}_z \sum_{n=1}^{\infty}\sum_{m=1}^{\infty} \frac{I_0}{j\omega\epsilon_0 ab\gamma_{mn}} \sin\left(\frac{n\pi x_1}{a}\right)\sin\left(\frac{m\pi y_1}{b}\right) \cdot\sin\left(\frac{n\pi x}{a}\right)\sin\left(\frac{m\pi y}{b}\right)\left[e^{-\gamma_{mn}z}k\sin\left(k(z_1+x_1)\right) - e^{-\gamma_{mn}z_1}\left(\gamma_{mn}\cos(kx_1)+k\sin(kx_1)\right)\cosh(\gamma_{mn}z)\right] \quad (9a)$$

$$\vec{E}_x = \vec{a}_x \sum_{n=0}^{\infty}\sum_{m=1}^{\infty} \frac{2I_0\delta_n}{jab\gamma_{mn}}\sqrt{\frac{u_0}{\epsilon_0}} \cos\left(\frac{n\pi x}{a}\right) \cdot\sin\left(\frac{m\pi y}{b}\right)e^{-\gamma_{mn}z} \cdot\sin\left(\frac{m\pi y_1}{b}\right)\sinh(\gamma_{mn}z_1)\left[\frac{n\pi}{ak}\sin(kx_1)\sin\left(\frac{n\pi y_1}{a}\right) - \sin(kx_1)\cos\left(\frac{n\pi x_1}{a}\right)\right]. \quad (9b)$$

The electric fields E_z and E_x are expressed in the form of Fourier series, where ω is the angular frequency, ϵ_0 is the permittivity, and $\sqrt{u_0/\epsilon_0}$ is the impedance of the medium.

D. The Input Impedance of the End Launcher

The input impedance seen by the microstrip line driven by the L-shaped current loop is obtained through the following equation [4]:

$$z_{\text{in}} = -\int_V \frac{\vec{E}_z\cdot\vec{J}_z}{I_{\text{in}}^2}\,dV - \int_V \frac{\vec{E}_x\cdot\vec{J}_x}{I_{\text{in}}^2}\,dV. \quad (10)$$

The first and the second term on the right-hand side of (10) are the input impedance due to the z-directed and x-directed currents, respectively. E_z and E_x are the electric fields inside the waveguide due to the currents J_z and J_x distributed over the volume V, and I_{in} is the total input current at the reference plane $z=0$. The quantities J_z, J_x, E_z, and E_x are given in (4a), (4b), (9a), and (9b). The product $E\cdot J$ must be integrated over the volume V. I_{in} is determined by performing the integration of the current density over a finite width of $2w$. By an expansion of (10), the integrands are reduced to their closed-form expres-

sions:

$$-\int_V \frac{\vec{E}_z\cdot\vec{J}_z}{I_{\text{in}}^2}\,dV = j\sum_{n=1}^{\infty}\sum_{m=1}^{\infty}\frac{1}{\omega\epsilon_0 ab\gamma_{mn}\cos^2(k(z_1+x_1))}\frac{a}{n\pi w}\sin\left(\frac{n\pi w}{a}\right)\sin^2\left(\frac{m\pi y_1}{b}\right)\sin^2\left(\frac{n\pi x_1}{a}\right)\left[\frac{k\sin(k(z_1+x_1))}{k^2+\gamma_{mn}^2}\right.$$
$$\cdot\left(\gamma_{mn}\cos(k(z_1+x_1))+k\sin(k(z_1+y_1))-e^{-\gamma_{mn}z_1}(\gamma_{mn}\cos(kx_1)+k\sin(kx_1))\right.$$
$$\left.\left.-\left(\frac{e^{-\gamma_{mn}z_1}(\gamma_{mn}\cos(kx_1)+k\sin(kx_1)}{k^2+\gamma_{mn}^2}(k\sin(k(z_1+y_1))+\gamma_{mn}\cos(kx_1)\sinh(\gamma_{mn}z_1)-k\sin(kx_1)\cosh(\gamma_{mn}z_1))\right)\right] \tag{11a}$$

$$-\int_V \frac{\vec{E}_x\cdot\vec{J}_x}{I_{\text{in}}^2}\,dV = j\sum_{n=0}^{\infty}\sum_{m=1}^{\infty}\frac{240\pi\delta_n}{abk\gamma_{mn}}\frac{\sinh(\gamma_{mn}w)}{\gamma_{mn}w}\sin^2\left(\frac{m\pi y_1}{b}\right)\sinh(\gamma_{mn}z_1)$$
$$\cdot e^{-\gamma_{mn}z_1}\frac{\left[\sin(kx_1)\cos\left(\frac{n\pi x_1}{a}\right)-\frac{n\pi}{ak}\cos(kx_1)\sin\left(\frac{n\pi x_1}{a}\right)\right]^2}{\cos^2(k(z_1+x_1))\left(1-\left(\frac{n\pi}{ak}\right)^2\right)}. \tag{11b}$$

The real part of the input impedance of the end launcher is contributed by the dominant mode; the higher order modes contribute to the reactive part only. This is expected in the latter case because the higher order modal fields are evanescent.

E. Reflection Coefficient of the End Launcher in a Back-to-Back Configuration

The input reflection coefficient amplitude at the reference plane $z=0$ in the microstrip line is determined through the equation

$$|\Gamma| = \sqrt{\frac{(R_{\text{in}}-Z_0)^2+X_{\text{in}}^2}{(R_{\text{in}}+Z_0)^2+X_{\text{in}}^2}} \tag{12}$$

where Z_0 is the characteristic impedance of the input microstrip line. R_{in} and X_{in} are the real and imaginary parts of the total input impedance Z_{in}.

When the two end launchers are connected back-to-back, the input reflection coefficient amplitude is redefined as

$$|\Gamma| = \sqrt{\frac{(R_{\text{in}}-R_1)^2+(X_{\text{in}}-X_1)^2}{(R_{\text{in}}+R_1)^2+(X_{\text{in}}+X_1)^2}} \tag{13a}$$

where R_1 and X_1 are given in the following forms:

$$R_1 = Z_0\frac{R_{\text{in}}(Z_0-X_{\text{in}}\tan(2\beta l))+R_{\text{in}}\tan(2\beta l)(X_{\text{in}}+Z_0\tan(2\beta l))}{(Z_0-X_{\text{in}}\tan(2\beta l))^2+(R_{\text{in}}\tan(2\beta l))^2} \tag{13b}$$

$$X_1 = Z_0\frac{(X_{\text{in}}+Z_0\tan(2\beta l))(Z_0-X_{\text{in}}\tan(2\beta l))-R_{\text{in}}^2\tan(2\beta l)}{(Z_0-X_{\text{in}}\tan(2\beta l))^2+(R_{\text{in}}\tan(2\beta l))^2} \tag{13c}$$

where β is the propagating phase constant of the shielded microstrip line at the specified frequencies. Its value is determined through the spectral-domain technique [9]. l is the length of the lossless microstrip line between the 2 transitions.

III. Results

The microstrip line to waveguide end launcher has been studied for a number of cases. The physical dimensions of the width of the current strip and the size of the input waveguide are fixed throughout the calculation. W is chosen to be 0.185 mm, and standard *Ka*-band waveguide dimensions are used. A substrate 10 mil thick with a dielectric constant of 2.2 is used as the dielectric slab. The end launcher is matched into an input microstrip line with a characteristic impedance of 75.0 Ω. The values of m and n are chosen to be 10 to ensure the convergence of the input impedance. Figs. 2, 3, and 4 show the numerical data of the input impedance of the end launcher for three different cases, calculated at frequencies from 26.5 to 40.0 GHz. In all cases the values of x_1 and y_1 are fixed, and z_1 is varied from 1.50 to 3.00 mm in order to observe the behavior of the transition input impedance. A family of curves of the impedance is generated by varying the parameter z_1. It is observed that generally the resistive part is higher at the lower end of the waveguide band. A lower input resistance level can be realized by choosing the offset transition with $y_1 = 5.25$ mm. As the value of z_1 increases, the best-matched frequency of the end launcher shifts towards the lower end of the waveguide band. For the case of $x_1 = 2.625$ mm and $y_1 = 3.50$ mm, the reactive part of the input impedance of the end launcher remains quite flat over a broad band of frequencies before resonance occurs. The reactance changes from inductive to capactive at resonance and behaves in an opposite manner to what we observe in the other two cases. This effect is due to the

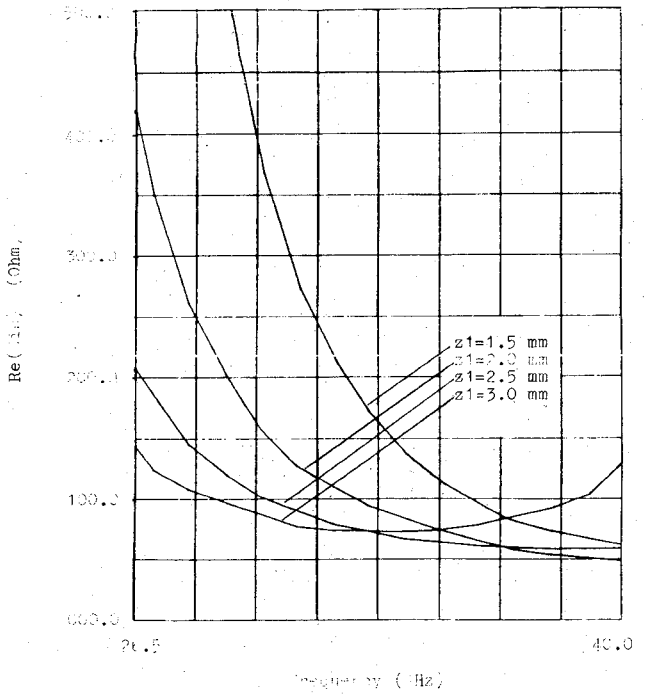

(a)

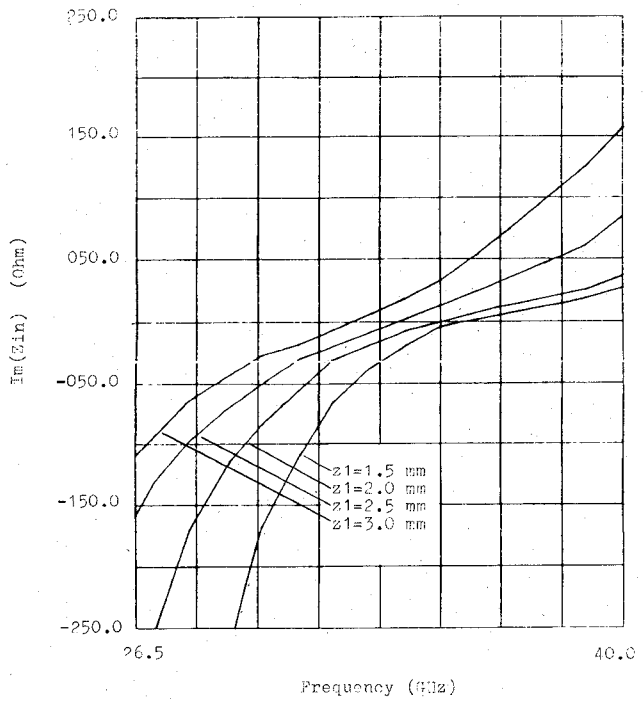

(b)

Fig. 2. Variation of the calculated input impedance versus frequency. Concentric end launcher with $x_1 = 1.75$ mm and $y_1 = 3.50$ mm. (a) Real part. (b) Imaginary part.

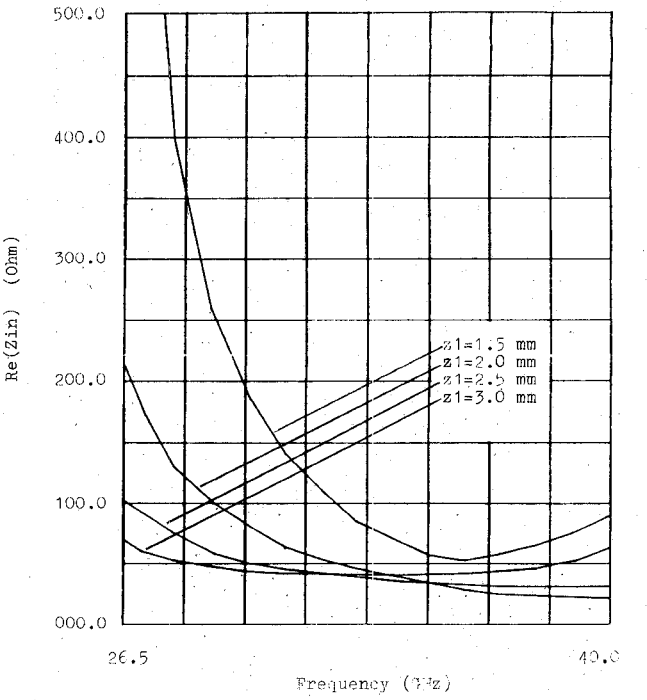

(a)

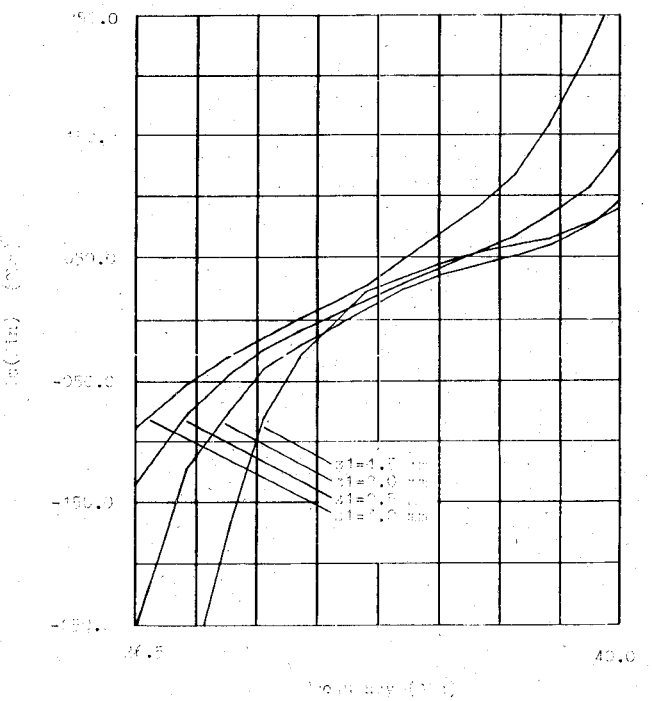

(b)

Fig. 3. Variation of the calculated input impedance versus frequency. Offset end launcher with $x_1 = 1.75$ mm and $y_1 = 5.25$ mm. (a) Real part. (b) Imaginary part.

proper cancellation of the reactances in the two arms of the current loop. To verify our calculation of the input impedance of the end launcher, we used the back-to-back reflection coefficient instead of direct measurement due to the difficulties involved in the experiment. The Z_{in} measurement would require a *Ka*-band vector network analyzer, and in addition, we would have to develop a reliable de-embedding computer program in order to extract the measured *S* parameters. Fig. 5 shows a *Ka*-band microstrip line to a waveguide end launcher circuit. A concentric end launcher was chosen for verification of the theory. The microstrip line to waveguide end launcher was

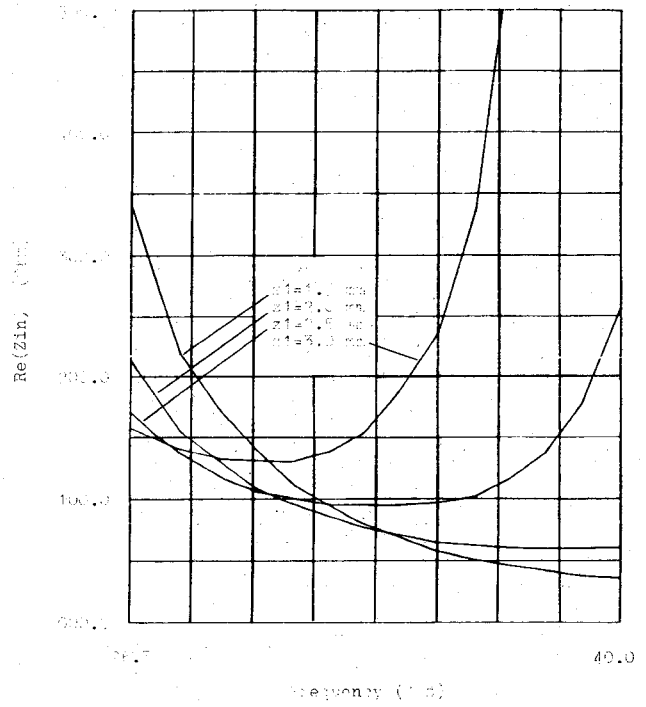

(a)

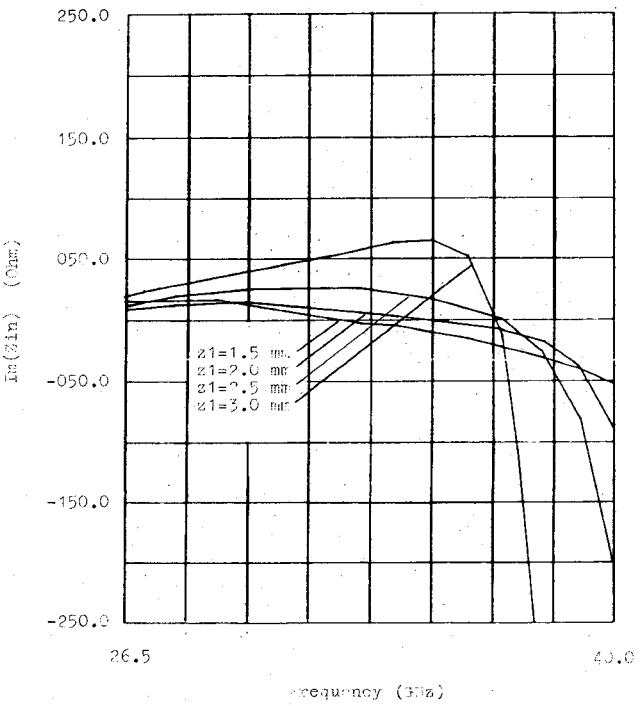

(b)

Fig. 4. Variation of the calculated input impedance versus frequency. Offset end launcher with $x_1 = 2.62$ mm and $y_1 = 3.50$ mm. (a) Real part. (b) Imaginary part.

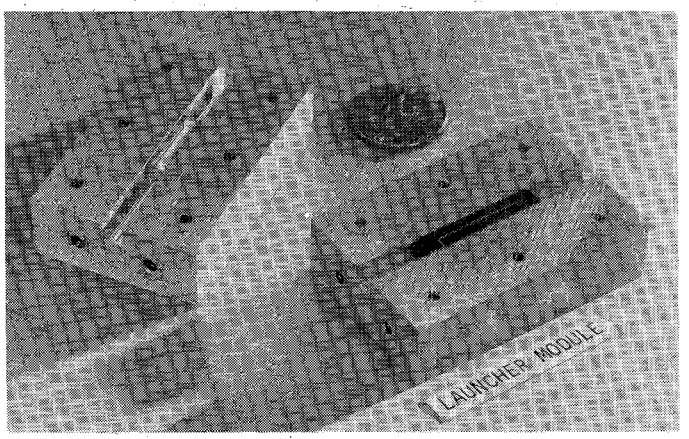

Fig. 5. *Ka*-band microstrip line-to-waveguide end launcher circuit.

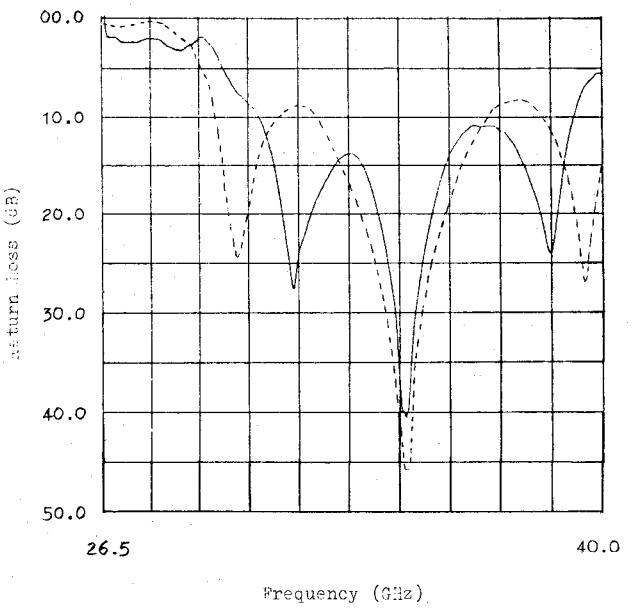

Fig. 6. Comparison between calculated and measured input return loss of the end launcher when 2 transitions are mounted in a back-to-back configuration. Concentric end launcher with $x_1 = 1.75$ mm, $y_1 = 3.50$ mm, and $z_1 = 2.00$ mm. ---- Theoretical. —— Experimental.

fabricated using Duroid substrate, and many circuits were tested for repeatability. Fig. 6 shows the calculated and typical measured input return loss for the case $x_1 = 1.75$ mm, $y_1 = 3.50$ mm, $z_1 = 2.00$ mm, and $l = 12.50$ mm when the two end launchers are mounted in a back-to-back configuration. The minima in the return loss data represent the phase cancellation of the multireflected signals in the circuit, while the maxima represent frequencies where the phases of the signals add. This behavior is observed only when the two end launchers, which are separated by a length of microstrip line, are in a back-to-back configuration. The comparison shows that the numerical calculations for the input return loss of the end launcher in general agree well with the experimental data. However, there is a small discrepancy for frequencies where the minima occurred in the return loss measurement. The difference may be due to the fact that we neglected the dielectric substrate and aperture effects in our analysis.

IV. Conclusions

The analysis of a microstrip line to waveguide end launcher has led to the development of a transition with low input return loss over a wide range of frequencies. The input impedance is computed using a stationary formula.

The analysis assumes a sinusoidal distribution existing in the current loop, which is true for an infinitesimally thin wire, instead of using an exact formula. A 45° chamfer is used to compensate the discontinuity of the current at the conductor bend. The effect of the exciting aperture is considered to be insignificant due to its small dimensions. However, it can be included in the analysis by taking into account the magnetic current existing over the aperture. Various cases have been evaluated and a comparison between input impedance measurement and theory shows good agreement at *Ka*-band frequencies.

References

[1] B. Glance and R. Trambarulo, "A waveguide to suspended stripline transition," *IEEE Trans. Microwave Theory Tech.*, vol. MTT-21, pp. 117–118, Feb. 1973.

[2] L. J. Lavedan, "Design of waveguide-to-microstrip transitions specially suited to millimeter-wave applications," *Electron. Lett.*, vol. 13, no. 20, pp. 604–605, Sept. 1977.

[3] R. E. Collin, *Field Theory of Guided Waves*. New York: McGraw-Hill, 1960, ch. 7, pp. 258–307.

[4] R. F. Harrington, *Time Harmonic Electromagnetic Field*. New York: McGraw-Hill, 1961, ch. 8, pp. 381–440.

[5] B. N. Das and G. S. Sanyal, "Coaxial-to-waveguide transition (end-launcher type)," *Proc. Inst. Elec. Eng.*, vol. 123, no. 10, pp. 984–986, Oct. 1976.

[6] M. D. Deshpande, B. N. Das, and G. S. Sanyal, "Analysis of an end launcher for an *X*-band rectangular waveguide," *IEEE Trans. Microwave Theory Tech.*, vol. MTT-27, pp. 731–735, Aug. 1979.

[7] C. T. Tai, *Dyadic Green's Functions in Electromagnetic Theory*. Scranton, PA: Haddon Craftsmen, 1971, ch. 5, pp. 76–80.

[8] W. L. Stutzman and G. A. Thiele, *Antenna Theory and Design*. New York: Wiley, 1981, ch. 2, pp. 87–92.

[9] T. Itoh and R. Mittra, "A technique for computing dispersion characteristics of shielded microstrip lines," *IEEE Trans. Microwave Theory Tech.*, vol. MTT-22, pp. 896–898, Oct. 1974.

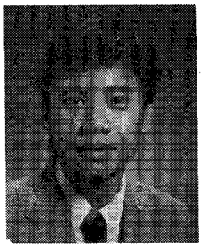

T. Q. Ho was born on January 11, 1961, in Saigon, Vietnam. He received the B.S.E.E. degree from Pennsylvania State University, University Park, in 1983 and the M.S.E.E. degree from California State University, Northridge, in 1987.

Prior to joining Hughes Aircraft Company in 1984, he was a microwave circuit designing engineer at Stable Energy Sources, Lancaster, PA. At Hughes Torrance Research Center, he has been involved in the research and development of advanced millimeter-wave integrated circuits based on FET's. Currently, he is a Senior Member of the Technical Staff at Hughes Space & Communications Group, where he is engaged in the development of flight RF modules and subsystems. His designing experience has included DRO's, VCO's, LNA's, filters, couplers, power dividers, and phase shifters. His present research interest is in solving waveguide excitation problems using numerical methods.

✠

Yi-Chi Shih (S'80–M'82) was born in Taiwan, Republic of China. He received the B.Sc. degree from the National Taiwan University, Taiwan, in 1976, the M.Sc. degree from the University of Ottawa, Ontario, Canada, in 1980, and the Ph.D. degree from the University of Texas at Austin in 1982, all in electrical engineering.

In September 1982, he joined the faculty at the Naval Postgraduate School, Monterey, CA, as an Adjunct Professor of Electrical Engineering. From April 1984 to May 1986, he was with the Hughes Aircraft Company, Microwave Products Division, Torrance, CA, as a Member of the Technical Staff. From May 1986 to May 1987, he was the Technical Director at the MM-Wave Technology, Inc., Torrance, CA. Since May 1987, he has been an independent technical consultant. His research interests include the application of numerical techniques to electromagnetic field problems and the modeling and development of millimeter-wave MIC and MMIC circuits.